Journal of
Applied and Computational Mechanics

Shahid Chamran
University of Ahvaz

Research Article

Vibration Analysis of Material Size-Dependent CNTs Using Energy Equivalent Model

Mohamed A. Eltaher[1,2], Mohamed Agwa[2], Abdallah Kabeel [2]

[1]Mechanical Engineering Dept., Faculty of Engineering, King Abdulaziz University,
P.O. Box 80204, Jeddah, Saudi Arabia

[2] Mechanical Design & Production Dept., Faculty of Engineering, Zagazig University,
P.O. Box 44519, Zagazig, Egypt

Abstract. This study presents a modified continuum model to investigate the vibration behavior of single and multi-carbon nanotubes (CNTs). Two parameters are exploited to consider size dependence; one derived from the energy equivalent model and the other from the modified couple stress theory. The energy equivalent model, derived from the basis of molecular mechanics, is exploited to describe size-dependent material properties such as Young and shear moduli for both zigzag and armchair CNT structures. A modified couple stress theory is proposed to capture the microstructure size effect by assisting material length scale. A modified kinematic Timoshenko nano-beam including shear deformation and rotary inertia effects is developed. The analytical solution is shown and verified with previously published works. Moreover, parametric studies are performed to illustrate the influence of the length scale parameter, translation indices of the chiral vector, and orientation of CNTs on the vibration behaviors. The effect of the number of tube layers on the fundamental frequency of CNTs is also presented. These findings are helpful in mechanical design of high-precision measurement nano-devices manufactured from CNTs.

Keywords: Energy Equivalent Model; Modified Couple Stress Theory; Carbon Nanotube; Vibration of Timoshenko Nano Beam; Analytical Model.

1. Introduction

Carbon nanotubes (CNTs), discovered by Iijima [1], have received wide attention in many scientific disciplines such as material science, engineering, and physics, because of their outstanding properties. CNT is considered as one of the most resilient and strongest material known. Carbon nanostructures such as single and multi-walled carbon nanotubes, nanofibers and nanoparticles are used greatly in the field of nanotechnology. The mechanical properties of CNTs are functions of both micro- and macro-mechanics. These functions can be derived through calculating the variation of microscopic electronic energies by the equivalent continuum energies, Tu and Ou-Yang [2]. Two theoretical approaches, such as molecular dynamics and continuum mechanics, are used to describe the behavior of CNTs accurately. Although Molecular dynamics is the most popular one in describing CNTs behavior [3], it is computationally expensive. Nowadays, Continuum mechanics approach is the subject of much research in nano-mechanics due to their computational accuracy and simplicity as compared to those results given by the atomistic model by Chen et al. [4].

The nano-beam has been used widely in systems and devices modeling such as nano-wires, nano-probes, CNTs, atomic force microscope (AFM), nano-actuators, and nano-sensors. According to Eltaher et al. [5], the understanding the vibrational behavior of the nano-beam is essential in developing such structures due to their great potential engineering applications.

Recently, many studies showed that the small length scale effect missing in the conventional continuum should be considered in the modelling of nanostructures. To overcome the size dependency problem in conventional continuum models, nano-continuum models were proposed including nonlocal theories as suggested by Eringen [6-8], the modified couple stress theory of [9-10], and the strain gradient theory [11-13]. All the above-mentioned theories described the length scale parameters as material constants. Conversely, the energy equivalent model, derived from combining molecular and continuum mechanics, described the properties of CNTs (i.e., Young's modulus, shear modulus, and Poisson's ratio) as size-dependent [14-17].

In 2005, Tserpes and Papanikos [18] proposed a 3D finite element model for single-walled carbon nanotubes (SWCNTs) that behave like space frame structures and determined their elastic moduli using both molecular and continuum mechanics. Wu et al. [14] presented the fundamental frequencies and mode shapes of SWCNTs numerically by using FE and Euler-Bernoulli beam (EBB) kinematics. Shokrieh and Rafiee [19], and Shodja and Delfani [20] predicted the elastic moduli of graphene sheets and CNTs using a linkage between the molecular structure and the equivalent frame structure. Bogacz and Noga [21] studied free transverse vibration analysis of a toothed gear. Ghavamian et al. [22] applied FE method to determine the shear modulus of single- and multi-walled CNTs directly from torsion tests. Based on the modified strain gradient elasticity and Bernoulli-Euler beam theories, Akgoz and Civalek [23] investigated the buckling problem of linearly tapered micro-columns. Feng et al. [24] predicted mechanical properties of carbon nano-springs by using molecular mechanics simulation. Within the Brenner interatomic potential and Fourier analysis, Pine et al. [25] exploited molecular dynamics to investigate flexural vibrational of SWCNTs with various lengths under different axial strains. Rafiee and Moghadam [26] conducted comprehensive review on the modeling and simulation of CNTs concentrating on buckling, vibrational, and thermal properties. Farrokhabadi et al. [27] investigated the effects of the Casimir force on the instability and adhesion of freestanding Cylinder–Plate and Cylinder–Cylinder geometries. Brischetto [28] and Sakharova et al. [17] used three-dimensional FE modeling to evaluate the tensile and bending rigidities, and subsequently, Young's moduli of non-chiral and chiral SWCNTs. Kiani [30] exploited Lennard-Jones potential function and nonlocal Rayleigh beam theory to investigate vibration behavior of orthogonal SWCNTs separated by van der Waals (vdW) forces.

Stölken and Evans [30] experimentally showed that the mechanical properties of the micro- /nano-structures were from their macro-scale. Thus, modified continuum models were proposed to consider the size effect of tiny structures in nano-scale size. One of the well-known theories is the couple stress theory developed by Mindlin et al. [9, 11, & 31] and Toupin [10]. Besides, Yang et al. [12] presented a modified couple theory that included a symmetric couple stress tensor and involved only one length scale parameter. Ma et al. [32] studied bending and vibration behavior of microstructure-dependent Timoshenko nano-beams. Fu and Zhang [33] studied the buckling of size-dependent microtubules using a modified couple theory. Ke and Wang [34] investigated vibration and instability of fluid-conveying DWNTs based on the modified couple stress theory and the Timoshenko beam theory. Based on the modified couple stress theory, Ghayesh et al. [35] presented the nonlinear dynamics behavior of a micro-beam. On the other hand, Tounsi et al. [36] studied the thermal buckling characteristics of DWCNTs using the nonlocal Timoshenko beam model. Benguediab et al. [37] and Semmah et al. [38] studied chirality and scale effects on the mechanical buckling of zigzag DWCNTs. Results showed that the buckling load is overestimated by the local beam if the scale effect is ignored for long NTs. Bazehhour et al. [39] studied free vibration of high-speed rotating Timoshenko shaft effect of centrifugally induced axial force. The Timoshenko beam is more applicable for short and stubby shafts especially at high speeds. Besseghier et al. [40] exploited the Winkler-type model to simulate the interaction of the zigzag SWCNTs with a surrounding elastic medium. The relation between deflection amplitudes and resonant frequencies of the SWCNTs was derived through the harmonic balance method. Akgöz and Civalek [41] studied bending response of non-homogenous micro-beams embedded in an elastic medium based on the modified strain gradient elasticity theory and in conjunction with various beam theories. Eltaher et al. [42] presented the nonlocal FE model to investigat the dynamic behavior of SWCNT resonators.

Fakhrabadi [43] presented a nonlinear dynamic behavior of CNTs nano-resonator using the couple stress theory and the Euler beam model. Akgöz and Civalek [44] illustrated static bending response of single-walled carbon nanotubes (SWCNTs) embedded in an elastic medium on the basis of higher-order shear deformation micro-beam models in conjunction with the modified strain gradient theory. Agwa and Eltaher [45] studied a surface effect on vibration behavior of carbyne nano-mechanical resonators by using the Timoshenko nano-beam. Eltaher et al. [46] presented a review on mechanical behavior of the nonlocal CNTs model as nano-beams. Eltaher et al. [47] illustrated the nonlinear static behavior of size-dependent and material-dependent nonlocal CNTs by using the nonlocal differential form of Eringen and the energy equivalent method. Civalek and Demir [48] presented a simple nonlocal beam model to study the buckling response of protein microtubules by using the nonlocal continuum theory and the Finite element procedure. Hamed et al. [49] investigated vibration characteristics of both nonlinear symmetric power and sigmoid functionally graded (FG) nonlocal nano-beams by using a nonlocal elasticity. Hosseini and Rahmani [50] investigated the thermal buckling and natural frequency of a curved functionally graded (FG) nano-beam in a thermal environment based on the Eringen's theory. Keivani et al. [51] studied the dynamic pull-in instability of cantilever nano-actuator fabricated from the conductive cylindrical nanowire with a circular cross-section under the presence of the Casimir force and surface effects. Sedighi [52] presented the impact of vibrational amplitude on the dynamic pull-in instability and fundamental frequency of actuated micro-beams by introducing the second order frequency–amplitude relationship. Keivani et al. [53, 54] exploited the modified couple stress theory to investigate the pull-in instability of paddle-type and double-sided NEMS sensors under the accelerating force. Wang et al. [55] illustrated large amplitude free vibration of electrically actuated nano-beams with surface energy and thermal effects.

To the best authors known, the vibration behavior of SWCNTs accompanying with the energy equivalent method and the modified couple stress has not yet been investigated. Therefore, the present study is intended to fill this gap in the literature by considering the energy equivalent method along with the modified couple Timoshenko nano-beam that accounts for both moderate rotation and rotary inertia which have not been considered in Euler Bernoulli assumptions. The paper structure is

arranged as follows: Section 2 depicts the linkage between molecular mechanics and continuum mechanics. Section 3 presents the basic formulation and mathematical model of SWCNTs modeled by the Timoshenko couple stress nano-beam. The analytical closed form solution of a mathematical model is also derived in Section 3. In Section 4, model validation and numerical results that showed the effects of chirality for both zigzag and armchair structures on the dynamic characteristics of SWCNTs are presented and discussed. Concluding remarks are summarized in Section 5.

2. Energy Equivalent Model of CNTs

The mathematical model describes the relationship between molecular mechanics and continuum mechanics of SWCNTs. Based on the molecular mechanics, CNTs properties are functions of both chiral angles and nanotube diameters. The chiral vector used to describe the chiral angle can be defined as [14]:

$$\vec{C}_h = n\vec{a}_1 + m\ \vec{a}_2 \tag{1}$$

where $\vec{a}_1$ and $\vec{a}_2$ are the unit vectors, and the integer pair (n,m) specifies the structure of carbon nanotubes. According to chiral vector $\vec{C}_h$, CNTs can be categorized as zigzag $(n,0)$, armchair (n,n), and chiral $(n,m \neq n$ or $0)$ structures. However, the radius of nanotube R can be depicted as a function of the integer pair (n,m) as suggested by Yamabe [56].

$$R = \frac{l_0\sqrt{3\left(n^2 + m^2 + nm\right)}}{2\pi} \tag{2}$$

where $l_0 = 0.142\ nm$ is the C-C bond length and n is the translation index. Regarding Eq. (2), the armchair and zigzag nanotubes radii can be presented as $3nl_0/2\pi$ and $\sqrt{3}nl_0/2\pi$, respectively. Carbon atoms have specific bond lengths and bond angles in a 3D space. These bonds can be described in terms of a potential energy as [26]:

$$U = U_L + U_\theta + U_\omega + U_T \tag{3}$$

where $U_L, U_\theta, U_\omega,$ and U_T are bond stretching, angle variation, inversion, and torsion energies, respectively . In case of tension and bending of SWCNs, the most significant energies are the bond stretching and angle energies. Therefore, Eq. (3) can be simplified to [14, 19]:

$$U = U_L + U_\theta = \frac{1}{2}\sum_i K_i \left(dR_i\right)^2 + \frac{1}{2}\sum_j C_j \left(d\theta_j\right)^2 \tag{4}$$

in which K_i is the stretching constant of the bond i, dR_i is the elongation of the bond i, C_j is the angle variance constant of the bond j, $d\theta_j$ is the variance of bond angle j. Table 1 presents formulas for Young modulus, Poisson's ratio and shear modulus as functions of geometrical dependent parameters [14, 57, & 58].

The parameters used in the analysis of armchair and zigzag orientations of SWCNTs are: the effective thickness of CNTs t=0.258 nm, the forces constants $K/2$ = 46900 kcal/mol/nm2, and C/2= 63 kcal/mol/rad^2. The effect of translation indices (n) on radii along with Young and shear moduli of both zigzag and armchair CNTs is illustrated in Fig. 1. As shown in this Fig., Young and shear moduli exhibit strong dependence on the translation index especially at smaller indices ($n \leq 10$) and this dependence becomes weak for large indices ($n >10$). In addition, the moduli of the armchair structure approaches to the graphite moduli (E_g, μ_g) faster than zigzag structure.

Table 1. Young and shear moduli for armchair and zigzag CNTs.

	Armchair structure (n,n)	Zigzag structure $(n,0)$
Young Modulus	$E_a = \dfrac{4\sqrt{3}}{3}\dfrac{KC}{3\,C\,t + 4\,K\,l_0^2\,t\left(\lambda_{a1}^2 + 2\,\lambda_{a2}^2\right)}$	$E_z = \dfrac{4\sqrt{3}KC}{9\,C\,t + 4\,K\,l_0^2\,t\left(\lambda_{z1}^2 + 2\,\lambda_{z2}^2\right)}$
Poisson's Ratio	$\upsilon_a = \dfrac{\lambda_{a1}l_0^2\,K - C}{\lambda_{a1}l_0^2\,K + 3C}$	$\upsilon_z = \dfrac{\lambda_{z1}l_0^2\,K + \sqrt{3}C}{\lambda_{z1}l_0^2\,K - 3\sqrt{3}C}$
Shear Modulus	$\mu_a = \dfrac{6\sqrt{3}\,KC}{\left(18\,C + K\,l_0^2\,\lambda_{a3}^2\right)t}$	$\mu_z = \dfrac{2\sqrt{3}\,KC}{\left(6\,C + 3K\,l_0^2\,\lambda_{z3}^2\right)t}$
Geometrical Parameters	$\lambda_{a1} = \dfrac{4 - cos^2\left(\pi/2n\right)}{16 + 2cos^2\left(\pi/2n\right)}$	$\lambda_{z1} = \dfrac{-3\sqrt{4 - 3\,cos^2\left(\pi/2n\right)}\ cos\left(\pi/2n\right)}{8\sqrt{3} - 2\sqrt{3}cos^2\left(\pi/2n\right)}$
	$\lambda_{a2} = \dfrac{-\sqrt{12 - 3\,cos^2\left(\pi/2n\right)}\ cos\left(\pi/2n\right)}{32 + 4cos^2\left(\pi/2n\right)}$	$\lambda_{z2} = \dfrac{12 - 9\,cos^2\left(\pi/2n\right)}{16\sqrt{3} - 4\sqrt{3}cos^2\left(\pi/2n\right)}$
	$\lambda_{a3} = \sqrt{\dfrac{4}{cos^2\left(\pi/2n\right)} - 1}$	$\lambda_{z3} = \sqrt{\dfrac{4}{3cos^2\left(\pi/2n\right)} - 1}$

According to Tu and Ou-Yang [2], the Young's modulus of multi-walled carbon nanotubes (MWCNTs) can be expressed as

a function of SWCNTs parameters, layer number N , and layer distance h as suggested by Benguediab et al. [37]:

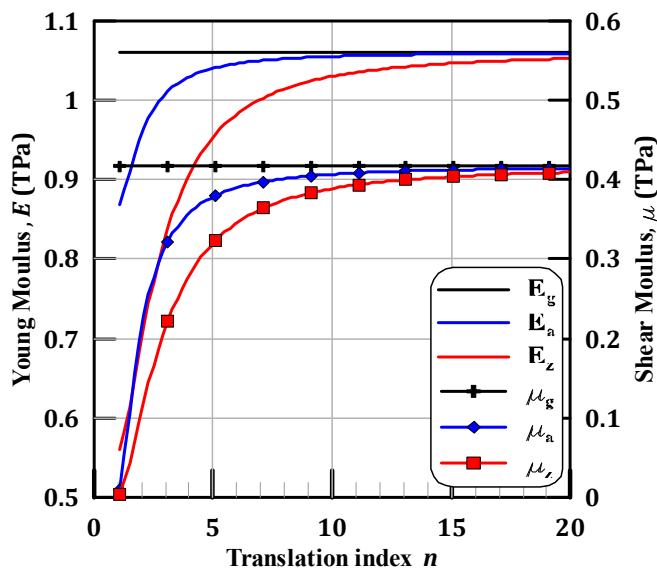$$E_{MWCNT} = \frac{N}{N-1+\dfrac{t}{h}} \frac{t}{h} E_{SWCNT} \tag{5}$$

Fig. 1. Variation of Young and shear moduli versus the translation index (n).

3. Problem Formulation

According to the modified couple stress theory, the elastic strain energy U can be described as suggested by Ma et al. [32]:

$$U = \frac{1}{2} \int_{\Omega} (\boldsymbol{\sigma} : \boldsymbol{\varepsilon} + \boldsymbol{m} : \boldsymbol{\chi}) dv \tag{6}$$

where Ω is the occupying region with a volume element dv, $\boldsymbol{\sigma}$, and $\boldsymbol{m}$ are a classical stress and couple stress tensors, $\boldsymbol{\varepsilon}$ and $\boldsymbol{\chi}$ are the classical strain and curvature strain tensors. The constitutive equations of a modified couple stress can be written as:

$$\boldsymbol{\sigma} = \lambda \, tr(\boldsymbol{\varepsilon}) \mathrm{I} + 2\mu \boldsymbol{\varepsilon} \tag{7.a}$$

$$\boldsymbol{m} = 2l^2 \mu \boldsymbol{\chi} \tag{7.b}$$

and subjected to the following geometrical fit conditions:

$$\boldsymbol{\varepsilon} = \frac{1}{2} \left[(\nabla \boldsymbol{u}) + (\nabla \boldsymbol{u})^T \right] \tag{8.a}$$

$$\boldsymbol{\chi} = \frac{1}{2} \left[(\nabla \boldsymbol{\theta}) + (\nabla \boldsymbol{\theta})^T \right] \tag{8.b}$$

$$\boldsymbol{\theta} = \frac{1}{2} \mathrm{curl}(\boldsymbol{u}) \tag{8.c}$$

where λ and μ are Lame's constants, and l is a material length scale parameter. Mathematically, l is the square root of the fraction of the curvature modulus to the shear modulus. Physically, l is a property measuring the effect of the couple stress [9, 32, 59]. $\boldsymbol{u}$ and $\boldsymbol{\theta}$ are the displacement and rotation vectors, respectively. Lame's constants have the following relations:

$$\lambda = \frac{E\nu}{(1+\nu)(1-2\nu)} \tag{9.a}$$

$$\mu = \frac{E}{2(1+\nu)} \tag{9.b}$$

where E is the Young modulus and ν is the Poisson's ratio. According to the Timoshenko beam theory, the kinematics of displacement can be defined as:

$$u(x,z,t) = u_0(x,t) - z\psi(x,t) \tag{10.a}$$

$$w(x,z,t) = w_0(x,t) \tag{10.b}$$

where $u(x,z,t)$ and $W(x,z,t)$ are the displacement components in x an z directions, $u_0(x,t)$ and $w_0(x,t)$ are the x and z components of the displacement vector at $z=0$, and $\psi(x,t)$ is the angle of rotation of the cross-section around the y axis with respect to z axis, as shown in Fig 2.
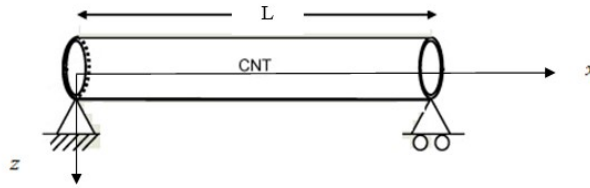

Fig. 2. Schematic representation of CNT beam.

By substituting Eq. (10) into Eq (8), the nonzero strains, rotation, and curvature have the following relations:

$$\varepsilon_{xx} = \frac{\partial u_0}{\partial x} - z \frac{\partial \psi}{\partial x} \tag{11.a}$$

$$\gamma_{xz} = \frac{\partial w}{\partial x} - \psi \tag{11.b}$$

$$\theta_y = -\frac{1}{2}\left[\psi + \frac{\partial w}{\partial x}\right] \tag{11.c}$$

$$\chi_{xy} = -\frac{1}{4}\left[\frac{\partial \psi}{\partial x} + \frac{\partial^2 w}{\partial x^2}\right] \tag{11.d}$$

Nonzero normal (σ_{xx}), shear (σ_{xz}), and couple (m_{xy}) stresses can be derived from Eqs. (7) as:

$$\sigma_{xx} = (\lambda + 2\mu)\varepsilon_{xx} = (\lambda + 2\mu)\left(\frac{\partial u_0}{\partial x} - z \frac{\partial \psi}{\partial x}\right) \tag{12.a}$$

$$\sigma_{xz} = \mu \gamma_{xz} = \mu\left(\frac{\partial w}{\partial x} - \psi\right) \tag{12.b}$$

$$m_{xy} = 2l^2 \mu \chi_{xy} = \frac{1}{2}l^2 \mu\left[\frac{\partial \psi}{\partial x} + \frac{\partial^2 w}{\partial x^2}\right] \tag{12.c}$$

The force and moment resultants can be described as follows:

$$N_x = \int_A \sigma_{xx} dA \tag{13.a}$$

$$M_x = \int_A z \, \sigma_{xx} dA \tag{13.b}$$

$$Y_{xy} = \int_A m_{xy} dA \tag{13.c}$$

$$Q = \int_A \sigma_{xz} dA \tag{13.d}$$

Based on the variation principle, the variation of strain energy δU, kinetic energy δK, and work δW done by a couple of Timoshenko beams can be determined as:

$$\delta U = \int_\Omega \left(\sigma_{xx}\delta\varepsilon_{xx} + \sigma_{xz}\delta\gamma_{xz} + 2m_{xy}\delta\chi_{xy}\right)dV$$

$$= \int_0^L \left[-\frac{\partial N_x}{\partial x}\delta u + \left(\frac{\partial M_x}{\partial x} - Q + \frac{1}{2}\frac{\partial \gamma_{xz}}{\partial x}\right)\delta\psi + \left(\frac{\partial Q}{\partial x} - \frac{1}{2}\frac{\partial^2 \gamma_{xz}}{\partial x^2}\right)\delta w \right]dx + \tag{14.a}$$

$$\left[N_x \delta u - \left(M_x - \frac{1}{2}\gamma_{xz}\right)\delta\psi + \left(Q + \frac{1}{2}\frac{\partial \gamma_{xz}}{\partial x}\right)\delta w - \frac{1}{2}\gamma_{xz}\frac{\partial w}{\partial x} \right]_0^L$$

$$\delta K = \int_0^L \left[m_0 \left(\frac{\partial^2 u}{\partial t^2} \delta u + \frac{\partial^2 w}{\partial t^2} \delta w \right) + m_2 \frac{\partial^2 \psi}{\partial t^2} \delta \psi \right] dx + \left[m_0 \left(\frac{\partial u}{\partial t} \delta u + \frac{\partial w}{\partial t} \delta w \right) + m_2 \frac{\partial \psi}{\partial t} \delta \psi \right]_0^L \tag{14.b}$$

$$\delta W = \int_0^L \left[f \, \delta u + q \, \delta w + c \, \delta \theta_y \right] dx + \left[\bar{N} \, \delta u + \bar{V} \, \delta w - \bar{M} \, \delta \delta \psi \right]_0^L \tag{14.c}$$

in which, L is the beam length, m_0 and m_2 are the translation and rotary inertia masses $m_0 = \int_A \rho dA$, $m_2 = \int_A z^2 \rho dA$, ρ is the mass density of the beam material, f and q are the distributed force in axial and transverse directions, respectively, and c is the body couple component in the y-direction per unit length along the x-axis. The bared symbols are the boundary forces and moments. By applying the Hamilton principle as:

$$\int_0^T \left[\delta K - \left(\delta U + \delta W \right) \right] dt = 0 \tag{15}$$

and substituting Eqs. (12) and (13) into Eq. (14) and consequently in Eq. (15), the modified couple equations of motion for the Timoshenko nano-beam may be presented in terms of displacements as:

$$\frac{EA(1-v)}{(1+v)(1-2v)} \frac{\partial^2 u_0}{\partial x^2} + f = m_0 \frac{\partial^2 u_0}{\partial t^2} \tag{16.a}$$

$$k_s \mu A \left(-\frac{\partial \psi}{\partial x} + \frac{\partial^2 w}{\partial x^2} \right) - \frac{1}{4} l^2 \mu A \left[\frac{\partial^3 \psi}{\partial x^3} + \frac{\partial^4 w}{\partial x^4} \right] + \frac{1}{2} \frac{\partial c}{\partial x} + q = m_0 \frac{\partial^2 w_0}{\partial t^2} \tag{16.b}$$

$$\frac{EI(1-v)}{(1+v)(1-2v)} \frac{\partial^2 \psi}{\partial x^2} + k_s \mu A \left(\frac{\partial w}{\partial x} - \psi \right) + \frac{1}{4} l^2 \mu A \left[\frac{\partial^2 \psi}{\partial x^2} + \frac{\partial^3 w}{\partial x^3} \right] - \frac{1}{2} c = m_2 \frac{\partial^2 \psi}{\partial t^2} \tag{16.c}$$

where $k_s = 6(1+v)^2 / \left(7 + 12v + 4v^2\right)$ is the Timoshenko shear coefficient. The system of Eqs. (16) is constrained by the following boundary conditions:

$$N_x = \bar{N} \qquad \qquad \text{or} \qquad u = \bar{u} \quad \text{at} \ \ x = 0 \ \& L \tag{17.a}$$

$$Q + \frac{1}{2} \frac{\partial Y_{xy}}{\partial x} + \frac{1}{2} c = \bar{V} \qquad \qquad \text{or} \qquad w = \bar{w} \quad \text{at} \ \ x = 0 \ \& L \tag{17.b}$$

$$M_x + \frac{1}{2} Y_{xy} = \bar{M} \qquad \qquad \text{or} \qquad \psi = \bar{\psi} \quad \text{at} \ \ x = 0 \ \& L \tag{17.c}$$

$$Y_{xy} = 0 \qquad \qquad \text{or} \qquad \frac{\partial w}{\partial x} = \overline{\frac{\partial w}{\partial x}} \quad \text{at} \ \ x = 0 \ \& L \tag{17.d}$$

To study the free vibrations of SWCNTs, the force terms [i.e., f, q, c and $\partial c / \partial x$] can be neglected from equations of motion because the in-plane displacement effect is insensitive with respect to transverse displacements. Therefore, the equations of motion for modified couple SWCNTs can be rewritten in a simplified form as follows:

$$k_s \mu A \left(-\frac{\partial \psi}{\partial x} + \frac{\partial^2 w}{\partial x^2} \right) - \frac{1}{4} l^2 \mu A \left[\frac{\partial^3 \psi}{\partial x^3} + \frac{\partial^4 w}{\partial x^4} \right] = m_0 \frac{\partial^2 w_0}{\partial t^2} \tag{18.a}$$

$$\frac{EI(1-v)}{(1+v)(1-2v)} \frac{\partial^2 \psi}{\partial x^2} + k_s \mu A \left(\frac{\partial w}{\partial x} - \psi \right) + \frac{1}{4} l^2 \mu A \left[\frac{\partial^2 \psi}{\partial x^2} + \frac{\partial^3 w}{\partial x^3} \right] = m_2 \frac{\partial^2 \psi}{\partial t^2} \tag{18.b}$$

In order to solve Eq. (18), the following expansions of generalized displacements w and ψ, which satisfy the boundary conditions in Eq. (17), are assumed as:

$$w(x,t) = \sum_{n=1}^{\infty} W_n \sin\left(\frac{n\pi x}{L} \right) e^{i\omega t} \tag{19.a}$$

$$\psi(x,t) = \sum_{n=1}^{\infty} \Psi_n \cos\left(\frac{n\pi x}{L} \right) e^{i\omega t} \tag{19.b}$$

where ω is the vibration frequency, and W_n and Ψ_n are the coefficients of Fourier series. By substituting the expansions of w and ψ provided in Eq. (19) into Eq. (18), we obtain the following equations:

$$\sum_{n=1}^{\infty}\left[k_s\mu A\left(\frac{n\pi\Psi_n}{L}-\frac{(n\pi)^2 W_n}{L^2}\right)-\frac{1}{4}l^2\mu A\left(\frac{(n\pi)^3\Psi_n}{L^3}+\frac{(n\pi)^4 W_n}{L^4}\right)+\omega^2 m_0 W_n\right]\sin\left(\frac{n\pi x}{L}\right)e^{i\alpha t}=0 \tag{20.a}$$

$$\sum_{n=1}^{\infty}\left[\frac{-EI(1-\nu)(n\pi)^2\Psi_n}{(1+\nu)(1-2\nu)L^2}+k_s\mu A\left(\frac{n\pi W_n}{L}-\Psi_n\right)-\frac{1}{4}l^2\mu A\left(\frac{(n\pi)^2\Psi_n}{L^2}+\frac{(n\pi)^3 W_n}{L^3}\right)+\omega^2 m_2\Psi_n\right]\cos\left(\frac{n\pi x}{L}\right)e^{i\alpha t}=0 \tag{20.b}$$

which can be rewritten in a matrix form as:

$$\begin{bmatrix}\dfrac{-(n\pi)^2 k_s\mu A}{L^2}-\dfrac{1}{4}\dfrac{(n\pi)^4 l^2\mu A}{L^4}+\omega^2 m_0 & \dfrac{n\pi k_s\mu A}{L}-\dfrac{1}{4}\dfrac{(n\pi)^3 l^2\mu A}{L^3} \\[2ex] \dfrac{n\pi k_s\mu A}{L}-\dfrac{1}{4}\dfrac{(n\pi)^3 l^2\mu A}{L^3} & \dfrac{-EI(1-\nu)(n\pi)^2}{(1+\nu)(1-2\nu)L^2}-k_s\mu A-\dfrac{1}{4}\dfrac{(n\pi)^2 l^2\mu A}{L^2}+\omega^2 m_2 \end{bmatrix}\begin{Bmatrix} W_n\sin\left(\dfrac{n\pi x}{L}\right) \\[2ex] \Psi_n\cos\left(\dfrac{n\pi x}{L}\right) \end{Bmatrix}e^{i\alpha t}=\begin{Bmatrix}0\\0\end{Bmatrix} \tag{21}$$

By equating the determinant of the coefficient matrix in Eq. (21) to zero, the fundamental frequencies of modified coupled SWCNTs can be described by:

$$\omega_n^2=\frac{-a_1+\sqrt{a_1^2-4a_2a_0}}{2a_2} \tag{22}$$

where the constants a_0, a_1, and a_2 are defined as:

$$a_0=\frac{-1}{4}\frac{(n\pi)^6 l^2\mu A\dfrac{EI(1-\nu)}{(2\nu^2+\nu+1)}+4(n\pi)^4\mu AL^2\left[l^2 k_s\mu A+k_s\dfrac{EI(1-\nu)}{(2\nu^2+\nu+1)}\right]}{L^6} \tag{23.a}$$

$$a_1=\frac{1}{4}\frac{\left\{4m_0 L^6 k_s\mu A+4(n\pi)^4 L^4\left[\mu A\left(m_0 k_s+\dfrac{1}{4}m_0 l^2\right)+m_0\dfrac{EI(1-\nu)}{(2\nu^2+\nu+1)}\right]+l^2\mu A(n\pi)^4 L^2 m_2\right\}}{L^6} \tag{23.b}$$

$$a_2=-m_0 m_2 \tag{23.c}$$

By substituting material properties of SWCNTs provided in Table 1 into Eq. (23), the fundamental frequencies of zigzag and armchair of SWCNTs derived from the energy equivalent model (EEM) can be computed. Moreover, the frequencies of double and multi-walled carbon nanotubes can be computed by using Table 1 and Eqs. (5), (22), and (23).

4. Numerical Results

This section is devoted to validate the proposed model with the published work. After that, the effects of translation indices, orientation, and length scale parameters on fundamental frequencies of modified couple SWCNTs derived from EEM are presented and discussed. The effect of translation index and material length scale on the fundamental frequency of double and multi-walled carbon nanotubes are also illustrated.

4.1 Validation

To validate the current model, the beam properties are assumed according to Ma et al. [32]. Fig. 3a presents the effect of length scale of the modified couple Timoshenko beam model on the 1st natural frequency for different Poisson's ratios. As shown, the fundamental frequency decreases by increasing the thickness to material length ratio (h/l) from 1 to 10. However, the frequency seems to converge to a constant value for thickness to material length ratio of greater than 10. This behavior indicates the fundamental frequency is size dependent in small regimes and is insensitive in macro regimes. These results are in agreement with the results presented by Ma et al. [32] as shown in Fig 3b.

4.2 Effects of translation indices

The effect of translation indices on the first four frequencies of SWCNTs at a length scale of $l=8.8\,nm$ for both armchair and zigzag structures is shown in Figs. 4a and 4b, respectively. As shown in these Figs, the fundamental frequencies decrease dramatically as the translation index (n) increases from 1 to 10 for both armchair and zigzag structures. However, for large values of translation index $(n>10)$, weak variation occurs in frequencies due to an increase in n. The fundamental frequencies for zigzag are higher than that for armchair.
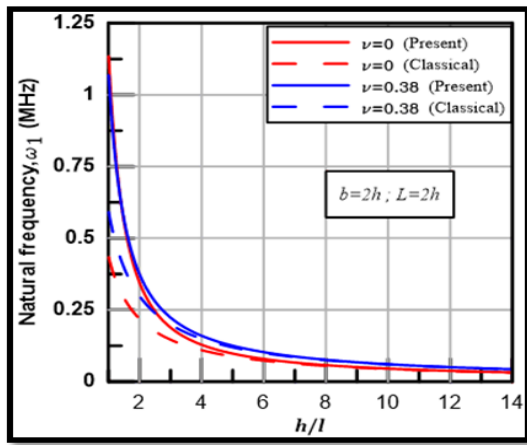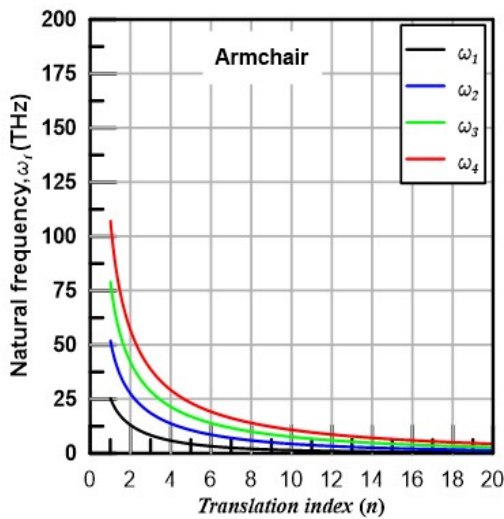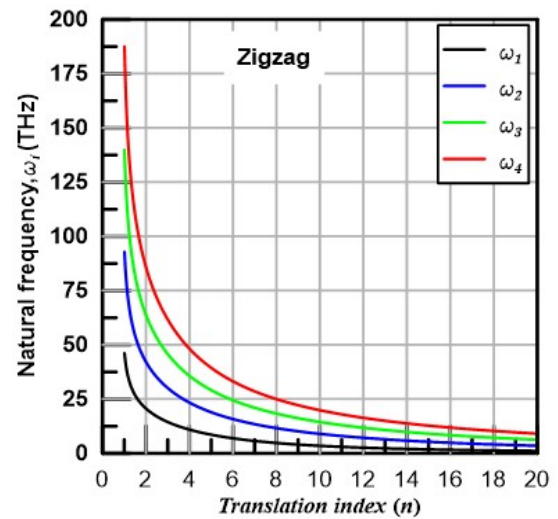
a) Present Analysis
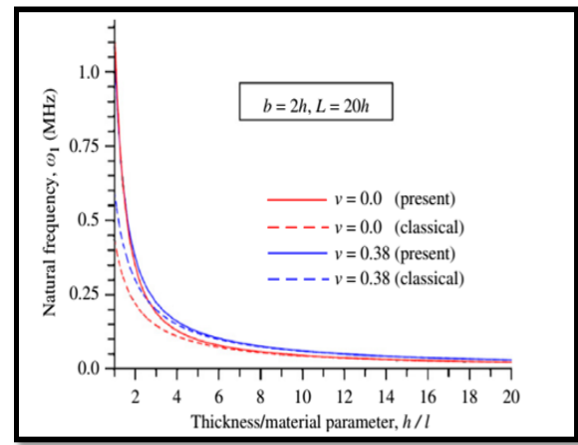
b) Fig 7 [Ma et al. [32]]

Fig. 3. Variation of 1st natural frequency versus h/l ratio for a modified and classical couple stress theory where h and b are the height and width of the beam.
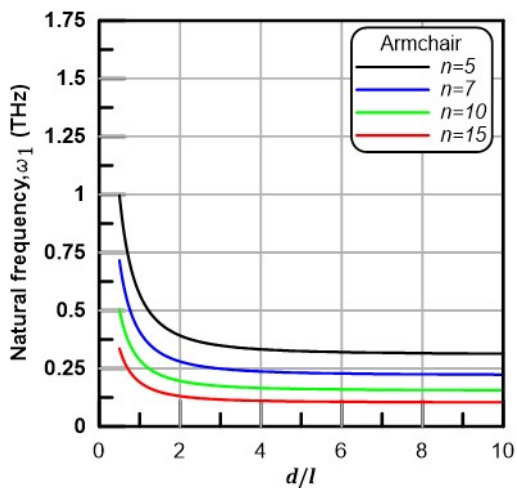

a) Armchair

b) Zigzag

Fig. 4. The effect of translation index on the first four frequencies of SWCNTs at $l = 8.8 \ nm$.

4.3 Length Scale Effect

The effects of material length scale on the 1st fundamental frequency of armchair and zigzag SWCNTs are presented in Figs.5 and 6, respectively. As can be concluded for both armchair and zigzag structures, the fundamental frequency decreases significantly by increasing the ratio of d/l from 1 to 3, where $d=2R$. However, the frequency is almost independent on ratio of diameter to material length scale in the region more than 4 at a specific translation index. This behavior is consistent with that proposed by Ma et al. [32].

a) Armchair
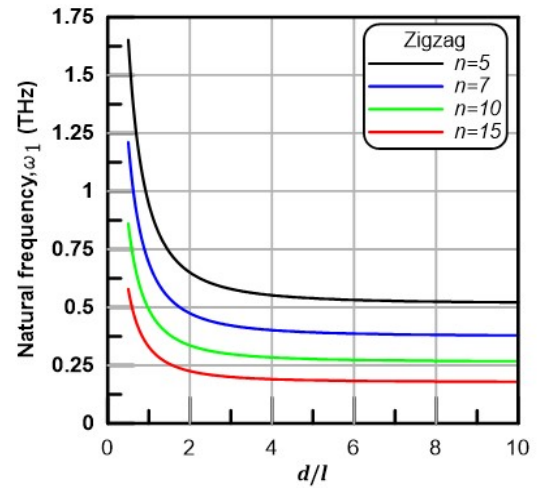
b) Zigzag

Fig. 5. The variation of the 1st fundamental frequency versus d/l ratio of SWCNTs at different translation indices

The effect of structure orientation on the fundamental frequency of SWCTs can be concluded from Fig 5. As shown, the fundamental frequency of zigzag orientation is higher than armchair orientation for the same translation index. This indicates that, the zigzag structure is stiffer than the armchair structure for the same translation index.

The relationship between the fundamental frequency and the translation index for armchair and zigzag SWCNTs at different material length scale is illustrated in Fig. 6. According to these Figs. it can be deduced that, as the length scale increases from 0.88 nm to 8.8 nm, the fundamental frequency increases. However, by a change in the length scale from 8.8 nm to 88 nm, a little bit increase in the fundamental frequency occurs especially where translation index (n) is more than 4. Therefore, in the analysis of vibrational behavior of CNTs, the length scale is more sensitive in the value length scale $l \leq 10\,nm$ and the modified coupled should be applied. If the value length scale $l \geq 10\,nm$, the classical theory may be applied.
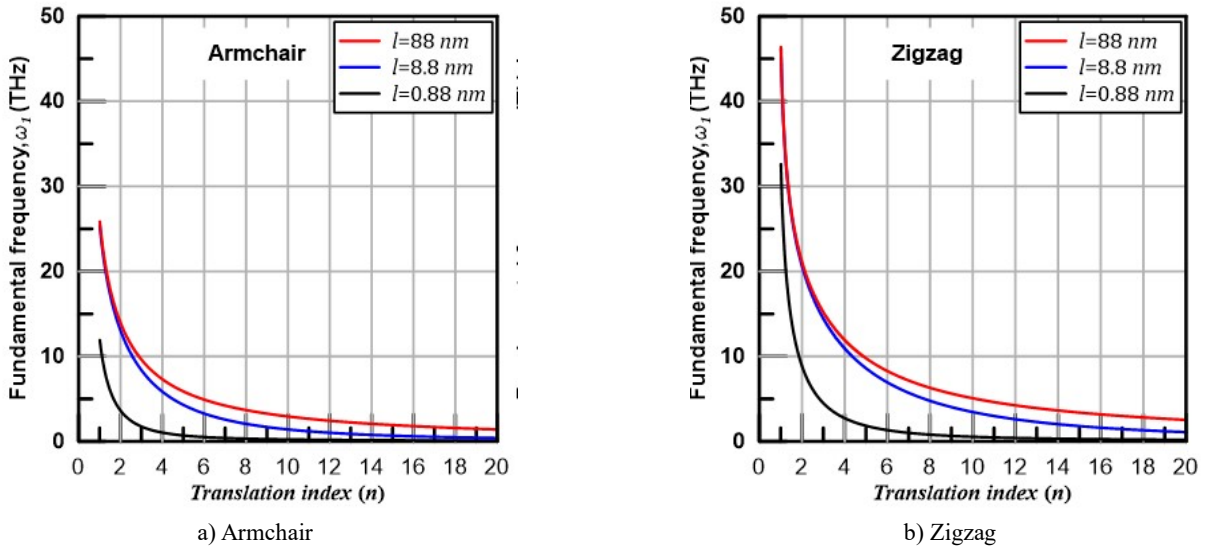

a) Armchair   b) Zigzag

Fig. 6. The variation of the 1st fundamental frequency versus translation index of SWCNTs at different material length scales

4.4 Number of Layer Effect

The variation in the fundamental frequency versus the translation index at a specific length scale $l = 8.8\,nm$ for single, double, and multi-carbon nanotubes is presented in Fig. 7. As illustrated, the fundamental frequency decreases as the number of layers increases. This observation is attributed to the reduction in CNT stiffness as the number of layers increases. The fundamental frequencies of multi-carbon nanotubes (MWCNTs), where N=3 and 4, are very close to each other. Therefore, it can be concluded that, the SWCNTs is stiffer than both DWCNTs and MWCNTs.
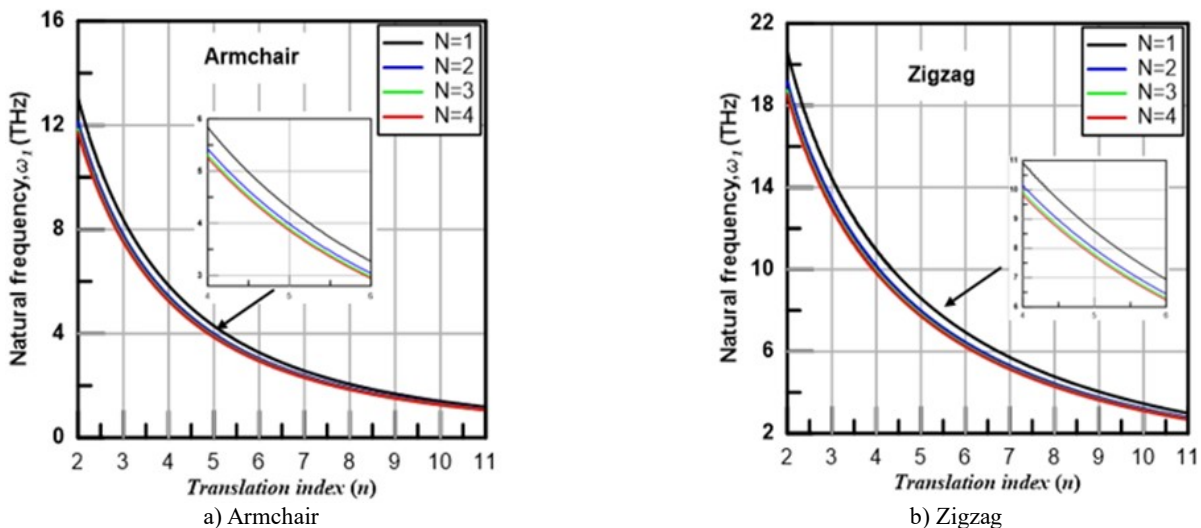

a) Armchair   b) Zigzag

Fig. 7. The effect of number of layers on the 1st fundamental frequency for single, double, and multi-walled carbon nanotubes at $l = 8.8\,nm$.

5. Conclusion

In this study, a modified continuum model was presented to explore and study the vibration behavior of single and multi-carbon nanotubes (CNTs). The energy equivalent model that derived from basis of molecular mechanics was exploited to depict the size-dependent material properties for both zigzag and armchair structures of CNTs. A modified couple stress theory was proposed to capture the microstructure size effect by assisting material length scale. A modified kinematic Timoshenko

nano-beam including shear deformation and rotary inertia effects was developed. Closed form expressions for natural frequencies were obtained and confirmed by previously published works. A parametric study was presented to illustrate the effects of the length scale parameter, translation indices of the chiral vector, number of tube layers, and CNTs orientation on the vibration behaviors of single and multi-carbon nanotubes. The main conclusions derived from the results are:

➢ Young and shear moduli exhibit strong dependence on the translation index especially at smaller indices.
➢ The fundamental frequencies decrease significantly as the translation index increases from 1 to 10 for both armchair and zigzag structures. The fundamental frequencies of zigzag are higher than that of armchair.
➢ For both armchair and zigzag structures, the fundamental frequency decreases significantly by increasing the ratio of d/l from 1 to 3.
➢ The fundamental frequency of zigzag orientation is higher than armchair orientation at the same translation index. This indicates that, the zigzag structure is stiffer than the armchair structure at the same translation index.
➢ The fundamental natural frequency decreases as the number of layers increases. This observation is due to the reduction in CNT stiffness as the number of layers increases. Therefore, it can be concluded that, the SWCNTs is stiffer than both DWCNTs and MWCNTs.

References

[1] Iijima, S., Helical microtubules of graphitic carbon, *Nature*, 354(6348), 1991, pp. 56-58.
[2] Tu, Z.C., Ou-Yang, Z.C., Single-walled and multiwalled carbon nanotubes viewed as elastic tubes with the effective Young's moduli dependent on layer number, *Physical Review B*, 65(23), 2002, pp. 233407.
[3] Haile, J.M., Molecular dynamics simulation: Elementary methods, *Computers in Physics*, 7(6), 1993, pp. 625-625.
[4] Chen Y., Lee J.D., Eskandarian. A., Atomistic viewpoint of the applicability of microcontinuum theories, *International Journal of Solids and Structures*, 41, 2004, pp. 2085-2097.
[5] Eltaher, M.A., Emam, S.A., Mahmoud, F.F., Free vibration analysis of functionally graded size-dependent nanobeams, *Applied Mathematics and Computation*, 218(14), 2012, pp. 7406-7420.
[6] Eringen, A.C., Nonlocal polar elastic continua, *International Journal of Engineering Science*, 10, 1972, pp. 1–16.
[7] Eringen A.C., On differential equations of nonlocal elasticity and solutions of screw dislocation and surface waves, *Journal of Applied Physics*, 54, 1983, pp. 4703–4710.
[8] Eringen, A.C., Nonlocal continuum field theories, New York: Springer-Verlag, 2002.
[9] Mindlin, R.D., Influence of couple-stresses on stress concentrations, *Experimental Mechanics*, 3(1), 1963, pp. 1-7.
[10] Toupin, R.A., Elastic materials with couple-stresses, *Archive for Rational Mechanics and Analysis*, 11(1), 1962, pp. 385-414.
[11] Mindlin, R.D., Eshel, N.N., On first strain-gradient theories in linear elasticity, *International Journal of Solids and Structures*, 4(1), 1968, pp. 109-124.
[12] Yang, F.A., Chong, A.C.M., Lam, D.C.C., Tong, P., Couple stress based strain gradient theory for elasticity, *International Journal of Solids and Structures*, 39(10), 2002, pp. 2731-2743.
[13] Lam, D.C.C., Yang, F., Chong, A.C.M., Wang, J., Tong, P., Experiments and theory in strain gradient elasticity, *Journal of the Mechanics and Physics of Solids*, 51(8), 2003, pp. 1477-1508.
[14] Wu, Y., Zhang, X., Leung, A.Y.T., Zhong, W., An energy-equivalent model on studying the mechanical properties of single-walled carbon nanotubes, *Thin-Walled Structures*, 44(6), 2006, pp. 667-676.
[15] Alizada, A.N., Sofiyev, A.H., Modified Young's moduli of nano-materials taking into account the scale effects and vacancies, *Meccanica*, 46, 2011, pp. 915–920.
[16] Rafiee, R., Moghadam, R.M., On the modeling of carbon nanotubes: a critical review, *Composites Part B: Engineering*, 56, 2014, pp. 435-449.
[17] Sakharova, N.A., Pereira, A.F.G., Antunes, J.M., Brett, C.M.A., Fernandes, J.V., Mechanical characterization of single-walled carbon nanotubes: Numerical simulation study, *Composites Part B: Engineering*, 75, 2015, pp. 73-85.
[18] Tserpes, K.I., Papanikos, P., Finite element modeling of single-walled carbon nanotubes, *Composites Part B: Engineering*, 36(5), 2005, pp. 468-477.
[19] Shokrieh, M.M., Rafiee, R., Prediction of Young's modulus of graphene sheets and carbon nanotubes using nanoscale continuum mechanics approach, *Materials & Design*, 31(2), 2010, pp. 790-795.
[20] Shodja, H.M., Delfani, M.R., A novel nonlinear constitutive relation for graphene and its consequence for developing closed-form expressions for Young's modulus and critical buckling strain of single-walled carbon nanotubes, *Acta mechanica*, 222(1-2), 2011, pp. 91-101.
[21] Bogacz, R., Noga, S., Free transverse vibration analysis of a toothed gear, *Archive of Applied Mechanics*, 82(9), 2012, pp. 1159-1168.
[22] Ghavamian, A., Rahmandoust, M., Öchsner, A., On the determination of the shear modulus of carbon nanotubes, *Composites Part B: Engineering*, 44(1), 2013, pp. 52-59.
[23] Akgoz, B., Civalek, O. Buckling analysis of linearly tapered micro-columns based on strain gradient elasticity, *Structural Engineering and Mechanics*, 48(2), 2013, pp. 195-205.
[24] Feng, C., Liew, K. M., He, P., Wu, A., Predicting mechanical properties of carbon nanosprings based on molecular mechanics simulation, *Composite Structures*, 114, 2014, pp. 41-50.
[25] Pine, P., Yaish, Y.E., Adler, J., Vibrational analysis of thermal oscillations of single-walled carbon nanotubes under axial strain, *Physical Review B*, 89(11), 2014, pp. 115405.

[26] Rappé, A.K., Casewit, C.J., Colwell, K.S., Goddard Iii, W.A., Skiff, W.M., A full periodic table force field for molecular mechanics and molecular dynamics simulations, *Journal of the American Chemical Society*, 114(25), 1992, pp. 10024-10035..

[27] Farrokhabadi, A., Abadian, N., Rach, R., Abadyan, M., Theoretical modeling of the Casimir force-induced instability in freestanding nanowires with circular cross-section, *Physica E: Low-dimensional Systems and Nanostructures*, 63, 2014, pp. 67-80.

[28] Brischetto, S., A continuum elastic three-dimensional model for natural frequencies of single-walled carbon nanotubes, *Composites Part B: Engineering*, 61, 2014, pp. 222-228.

[29] Kiani, K., Vibration analysis of two orthogonal slender single-walled carbon nanotubes with a new insight into continuum-based modeling of van der Waals forces, *Composites Part B: Engineering*, 73, 2015, pp. 72-81.

[30] Stölken, J.S., Evans, A.G., A microbend test method for measuring the plasticity length scale, *Acta Materialia*, 46(14), 1998, pp. 5109-5115.

[31] Mindlin, R.D., Tiersten, H.F., Effects of couple-stresses in linear elasticity, *Archive for Rational Mechanics and Analysis*, 11(1), 1962, pp. 415-448.

[32] Ma, H.M., Gao, X.L., Reddy, J.N., A microstructure-dependent Timoshenko beam model based on a modified couple stress theory, *Journal of the Mechanics and Physics of Solids*, 56(12), 2008, pp. 3379-3391.

[33] Fu, Y., Zhang, J., Modeling and analysis of microtubules based on a modified couple stress theory, *Physica E: Low-dimensional Systems and Nanostructures*, 42(5), 2010, pp. 1741-1745.

[34] Ke, L.L., Wang, Y.S., Flow-induced vibration and instability of embedded double-walled carbon nanotubes based on a modified couple stress theory, *Physica E: Low-dimensional Systems and Nanostructures*, 43(5), 2011, pp. 1031-1039.

[35] Ghayesh, M.H., Farokhi, H., Amabili, M., Nonlinear dynamics of a microscale beam based on the modified couple stress theory, *Composites Part B: Engineering*, 50, 2013, pp. 318-324.

[36] Tounsi, A., Benguediab, S., Adda, B., Semmah, A., Zidour, M., Nonlocal effects on thermal buckling properties of double-walled carbon nanotubes, *Advances in Nano Research*, 1(1), 2013, pp. 1-11.

[37] Benguediab, S., Tounsi, A., Zidour, M., Semmah, A., Chirality and scale effects on mechanical buckling properties of zigzag double-walled carbon nanotubes, *Composites Part B: Engineering*, 57, 2014, pp. 21-24.

[38] Semmah, A., Tounsi, A., Zidour, M., Heireche, H., Naceri, M., Effect of the chirality on critical buckling temperature of zigzag single-walled carbon nanotubes using the nonlocal continuum theory, *Fullerenes, Nanotubes and Carbon Nanostructures*, 23(6), 2015, pp. 518-522.

[39] Bazehhour, B.G., Mousavi, S.M., Farshidianfar, A., Free vibration of high-speed rotating Timoshenko shaft with various boundary conditions: effect of centrifugally induced axial force, *Archive of Applied Mechanics*, 84(12), 2014, pp. 1691-1700.

[40] Besseghier, A., Heireche, H., Bousahla, A.A., Tounsi, A., Benzair, A., Nonlinear vibration properties of a zigzag single-walled carbon nanotube embedded in a polymer matrix, *Advances in Nano Research*, 3(1), 2015, pp. 29-37.

[41] Akgöz, B., Civalek, Ö., Bending analysis of FG microbeams resting on Winkler elastic foundation via strain gradient elasticity, *Composite Structures*, 134, 2015, pp. 294-301.

[42] Eltaher, M.A., Agwa, M.A., Mahmoud, F.F., Nanobeam sensor for measuring a zeptogram mass, *International Journal of Mechanics and Materials in Design*, 12(2), 2016, pp. 211-221.

[43] Fakhrabadi, M.M.S., Prediction of small-scale effects on nonlinear dynamic behaviors of carbon nanotube-based nano-resonators using consistent couple stress theory, *Composites Part B: Engineering*, 88, 2016, pp. 26-35.

[44] Akgöz, B., Civalek, Ö., Bending analysis of embedded carbon nanotubes resting on an elastic foundation using strain gradient theory, *Acta Astronautica*, 119, 2016, pp. 1-12..

[45] Agwa, M.A., & Eltaher, M.A., Vibration of a carbyne nanomechanical mass sensor with surface effect, *Applied Physics A*, 122(4), 2016, pp. 1-8.

[46] Eltaher, M.A., Khater, M.E., Emam, S.A., A review on nonlocal elastic models for bending, buckling, vibrations, and wave propagation of nanoscale beams, *Applied Mathematical Modelling*, 40, 2016, pp. 4109–4128.

[47] Eltaher, M.A., El-Borgi S., Reddy J.N., Nonlinear Analysis of Size-dependent and Material-Dependent Nonlocal CNTs, *Composite Structure*, 153, 2016, pp. 902-913.

[48] Civalek, Ö., Demir, C., A simple mathematical model of microtubules surrounded by an elastic matrix by nonlocal finite element method, *Applied Mathematics and Computation*, 289, 2016, pp. 335-352.

[49] Hamed M.A., Eltaher M.A., Sadoun, A.M., Almitani K.H., Free vibration of Symmetric and Sigmoid Functionally Graded Nanobeams, *Applied Physics A: Materials Science and Processing*, 122(9), 2016, pp. 625-625.

[50] Hosseini, S.A.H., Rahmani, O., Thermomechanical vibration of curved functionally graded nanobeam based on nonlocal elasticity, *Journal of Thermal Stresses*, 39(10), 2016, pp. 1252-1267.

[51] Keivani, M., Mardaneh, M., Koochi, A., Rezaei, M., Abadyan, M., On the dynamic instability of nanowire-fabricated electromechanical actuators in the Casimir regime: Coupled effects of surface energy and size dependency, *Physica E: Low-dimensional Systems and Nanostructures*, 76, 2016, pp. 60-69.

[52] Sedighi, H.M., Size-dependent dynamic pull-in instability of vibrating electrically actuated microbeams based on the strain gradient elasticity theory, *Acta Astronautica*, 95, 2014, pp. 111-123.

[53] Keivani, M., Khorsandi, J., Mokhtari, J., Kanani, A., Abadian, N., Abadyan, M., Pull-in instability of paddle-type and double-sided NEMS sensors under the accelerating force, *Acta Astronautica*, 119, 2016, pp. 196-206.

[54] Keivani, M., Mokhtari, J., Abadian, N., Abbasi, M., Koochi, A., Abadyan, M., Analysis of U-shaped NEMS in the Presence of Electrostatic, Casimir, and Centrifugal Forces Using Consistent Couple Stress Theory, *Iranian Journal of Science and Technology, Transactions A: Science*, 2017, doi: 10.1007/s40995-017-0151-y.

[55] Wang, K.F., Zeng, S., Wang, B.L., Large amplitude free vibration of electrically actuated nanobeams with surface energy

and thermal effects, *International Journal of Mechanical Sciences*, 131–132, 2017, pp. 227-233.

[56] Yamabe, T., Recent development of carbon nanotube, *Synthetic Metals*, 70(1), 1995, pp. 1511-1518

[57] Baghdadi, H., Tounsi, A., Zidour, M., Benzair, A., Thermal Effect on Vibration Characteristics of Armchair and Zigzag Single-Walled Carbon Nanotubes Using Nonlocal Parabolic Beam Theory, *Fullerenes, Nanotubes and Carbon Nanostructures*, 23(3), 2015, pp. 266-272.

[58] Eltaher, M.A., Agwa, M.A., Analysis of Size-dependent Mechanical Properties of CNTs Mass Sensor Using Energy Equivalent Model, *Sensor and Actuator A: Physical*, 246, 2016, pp. 9-17.

[59] Park, S.K., Gao, X.L., Bernoulli–Euler beam model based on a modified couple stress theory, *Journal of Micromechanics and Microengineering*, 16(11), 2006, pp. 2355.